



# Linear Collider Collaboration Tech Notes

---

## Matching Program for the NLC Main Linac

August 31, 1999

Yuri Nosochkov, Tor Raubenheimer  
and Mark Woodley

Stanford Linear Accelerator Center  
Stanford, California

***Abstract:***

In this note, we describe the computer code used to design the NLC main linac optics, and present the current parameters of the linac lattice.

# Matching Program for the NLC Main Linac

Yuri Nosochkov, Tor Raubenheimer and Mark Woodley  
Stanford Linear Accelerator Center, Stanford University, Stanford, CA 94309

## Abstract

In this note, we describe the computer code used to design the NLC main linac optics, and present the current parameters of the linac lattice.

## 1 Introduction

The two main components of the linac are accelerator structures for beam acceleration and quadrupoles for transverse focusing. Most of the NLC linac length is occupied by the accelerator structures with the combined length of about 9 km to attain a design energy of 500 GeV with a loaded accelerating gradient of 55 MeV/m. The main requirements for the quadrupole system include: focusing of the beam transverse dimensions, minimization of various emittance dilution effects and providing optimal conditions for beam diagnostics.

The present design is based upon FODO cells with the F and D quadrupoles separated by an integral number of accelerator structures. Compared to other choices, the FODO system uses less quadrupole length and simplifies the engineering design. In comparison with a doublet optics (FDOFDO), the FODO system has looser tolerances on rms quad misalignment [1].

The choice of the FODO cell parameters is based upon minimization of various emittance dilution effects. Dispersive, chromatic and quadrupole vibration effects are reduced in a weaker focusing system, but the transverse wakefield effects are easier to compensate in a stronger lattice (see, for example, discussions of linac dynamics at Ref. [2]). As a function of energy, the wakefield compensation requires a stronger focusing at low energies, while the beam size can be gradually increased with beam acceleration. One natural scaling for the lattice is to maintain a constant energy spread for BNS autophasing wakefield compensation. In this case, the cell length (and  $\beta$  functions) can be increased with energy as  $\sim \sqrt{E}$ . The increased spacing also reduces the combined linac quadrupole length.

To minimize the linac length without introducing length variations of individual accelerator structures and to simplify the design, the increase in cell length with energy is made in a step-wise fashion. The full linac is divided into three sections with fixed cell length in each section and with 3, 6 and 9 accelerator structures per half-cell in the 1st, 2nd and the 3rd sections, respectively. For linac acceleration from 10 to 500 GeV the transitions between the three sections are made at about 50 and 155 GeV to satisfy approximately  $L_{cell} \sim \sqrt{E}$ . Another option of having 5 linac sections with 2, 4, 6, 8, and 10 structures per half-cell, similar to that discussed in the ZDR [3], resulted in somewhat larger emittance dilution due to dispersive effects [1].

Within each linac section, with constant cell length, the focusing can be gradually reduced by use of other means, i.e. by reducing the cell phase advance with energy. In the current design we use the following phase variation:

$$\mu = \mu_0(E/E_0)^a, \tag{1}$$

where  $\mu$  and  $E$  are the cell phase advance and beam energy, index “0” refers to the beginning of each section, and  $a = -0.3$  in the 1st and 2nd sections and  $a = 0$  in the 3rd section.

## 2 Linac Matching Program

The  $\beta$  functions in the array of identical FODO cells have high periodicity which helps reduce effects of chromatic and systematic focusing errors on emittance growth. The periodic solutions for the FODO cells are easy to find, however the complexity of the linac matching is due to energy changes and phase variation from cell-to-cell (Eq. 1). The beam acceleration results in each quadrupole having a distinct magnetic field and leads to variation of optical effect of accelerator structures along the linac. As a result, each cell needs to be matched individually.

There are a few hundred cells in the linac which makes it time consuming for a manual matching of each cell. The conventional optics codes such as MAD [4], in principle, allow to match all cells at once, but a lot of manual work is required to prepare the deck and set hundreds of matching conditions. In addition, the NLC naming convention requires the quadrupoles to be named sequentially, according to their position, for instance: QQ0101, QQ0102, QQ0103, ..., etc. In this case, even a small lattice modification might require significant amount of work just to rename the elements.

To automate the linac lattice setup and cell matching, a special linac matching code was developed [5]. For given linac parameters, this code generates the complete lattice including quadrupoles, accelerator structures,  $x$  and  $y$  orbit correctors and double view BPMs; applies proper names to the elements; executes cell-by-cell matching; generates and matches transitions between linac sections; creates MAD compatible lattice file; calculates lattice functions, BNS autophasing energy spread and ground motion tolerances due to quadrupole vibrations, dispersive and wakefield effects. The latest version of this code can be found at:

`"/afs/slac.stanford.edu/g/nlc/codes/linac/source,"`

where "linac\_08.f" and "linac\_subs.f" contain the Fortran code and "linac\_08" is the executable file.

### 2.1 Input Data

Upon executing the "linac\_08" file, the code will interactively ask for the data on the number of particles per bunch, accelerator gradient and final energy. For instance:

```
Input N[part/bunch], RFgrad[GeV/m], final energy[GeV]
> 1.1d10 0.055 500.
```

Secondly, the code will ask for a file containing the data on required lattice parameters. The name of this file has to be in the form of "linac\_08.filename.input", where "filename" can be any word and has to be used in response for the file name request. For example:

```
Input Filename [" " = no files output]
> filename
```

The data in the "filename" input file has to be arranged in a table with one row for each linac section (in sequential order) and 10 columns for the following parameters:

1. S-position of the beginning of the section, where  $s = 0$  is the beginning of linac (m).
2. S-position of the end of the section (m).
3. Number of accelerator structures per half-cell.
4. Half-length of a cell quadrupole (m).
5. Space between a quadrupole and adjacent accelerator structure (m).

6. Space between accelerator structures (m).
7. Horizontal cell phase advance in the beginning of the section (deg).
8. Vertical cell phase advance in the beginning of the section (deg).
9. Exponential factor  $a$  for horizontal cell phase advance (Eq. 1).
10. Exponential factor  $a$  for vertical cell phase advance (Eq. 1).

A comment can be placed after the 10th column. An example of such an input file is given below:

```

0.    881.  3  .16510  .159385  0.106680  100.0  105.0  -.3  -.3  Sector 1
881.  3101. 6  .21910  .267310  0.150368  100.0  105.0  -.3  -.3  Sector 2
3101. 10387. 9  .48895  .159385  0.161290   85.0   90.0  -.0  -.0  Sector 3

```

Some other linac parameters are defined in the code. They are: the initial beam energy (10 GeV), the length of individual accelerator structures (1.8025 m), the initial horizontal and vertical emittances ( $3 \cdot 10^{-6}$  and  $3 \cdot 10^{-8}$  m-rad), the rms bunch length (150  $\mu\text{m}$ ) and the wakefield strength.

## 2.2 Cell Model

The code will create each individual cell in the following sequence of elements:

- half of an F-quad (horizontally focusing),
- drift between the F-quad and the accelerator structure,
- accelerator structure,
- drift between structures,
- ... *repeat* "structure-drift" sequence according to the number of structures ...,
- accelerator structure,
- drift between the structure and the D-quad,
- first half of the D-quad (vertically focusing),
- double view BPM ( $L = 0$ ),
- vertical orbit corrector ( $L = 0$ ),
- second half of the D-quad,
- drift between the D-quad and the accelerator structure,
- accelerator structure,
- drift between structures,
- ... *repeat* "structure-drift" sequence according to the number of structures ...,
- accelerator structure,
- drift between the structure and the F-quad,
- half of the F-quad,
- double view BPM ( $L = 0$ ),
- horizontal orbit corrector ( $L = 0$ ),

where  $L = 0$  indicates a thin lens element. In addition to the above, the code will add one marker after each orbit corrector when creating the MAD compatible lattice file.

## 2.3 Lattice Generation

According to the input data, the code will sequentially generate the full lattice and match individual cells and transitions between sections when they are created. Each individual linac section will

be expanded with cells until it exceeds its specified length. Then a transition two-cell optics is generated to match the  $\beta$  functions to the next section. This procedure is repeated until all sections are generated. The initial linac  $\beta$  functions are defined as the initial periodic  $\beta$  values of the first linac cell with accelerator gradient set to zero. The optics match is aimed at providing the correct phase variation with energy (Eq. 1) and keeping the  $\beta$  functions as periodic as possible along the linac as it helps minimize emittance dilution due to chromatic and systematic quadrupole errors.

## 2.4 Cell Matching

Within each linac section, as defined in the input data, all cells have the same length, quadrupole length and number of accelerator structures. Therefore, the periodic optical solutions vary very little between subsequent cells, only due to variation of phase advance with energy (Eq. 1) and energy dependent focusing in the structures. This quasi-periodicity allows a simple cell-by-cell matching to be used.

For each individual cell, the strengths of the three cell quadrupoles (F/2 - D - F/2) are optimized. The main matching constraint is to achieve the correct  $x$  and  $y$  cell phase advance as a function of energy (Eq. 1). The use of three variable strengths allows inclusion of additional weak constraints (with small weight) to minimize the  $\alpha$  function ( $\alpha = -\frac{1}{2}\frac{d\beta}{ds}$ ) in the middle of quadrupoles and  $\beta$  variation from cell-to-cell. Since the  $\beta$  change from cell-to-cell is typically small, this match produces satisfactory quasi-periodic  $\beta$  functions along each linac section.

The above match results in slightly different strengths of the two halves of the F-quadrupoles. To equalize them in the MAD output lattice file, the code will average the strength over each quadrupole.

## 2.5 Automatic Transition Matching

Typically, different linac sections have different cell parameters such as cell length and phase advance. In general, the one cell match described in the previous section would not give a satisfactory optical transition between subsequent linac sections because of abrupt change in the cell parameters. To avoid large  $\beta$  perturbation one needs at least four independent quadrupoles to match the  $\beta$  and  $\alpha$  functions between the sections.

In the code, each transition optics is created in the following way. After the length of the current linac section is reached, two more cells of the same pattern (including structures) will be added and used for transition to the next section. In the transition matching, the code will optimize five quadrupole strengths of this two cell section (F/2 - D - F - D - F/2) to make an exact match for  $\beta$  and  $\alpha$  functions between the exit of the previous section and the entry to the next section. For the initial  $\beta$  functions of the new section the code will use the periodic  $\beta$  values of the first cell of this section with accelerator gradient set to zero. The five variables permit the use of an additional weak constraint to minimize  $\alpha$  function in the middle quadrupole of the transition section.

## 2.6 Manual Transition Optimization

Typically, the automatic transition matching provides adequate optics. In some cases, however, an additional optimization might be needed, for instance to reduce chromatic perturbation caused by abrupt change in periodicity. Since there are only a few transition sections per linac, the optimization can be done by using better matching capabilities of conventional codes such as MAD.

Since the linac code generates MAD compatible lattice file, it can be used for additional matching with MAD. Typically, one needs to vary a few more quadrupoles near transition sections and apply additional constraints to reduce chromatic perturbation (such optimization, for example, was done for SLC “stronger” lattice [6]).

## 2.7 Output

Upon completion, the code will produce summary output on the screen and save the detailed information in the output files. The screen output contains:

- The table which has one line of information for each cell with columns for element number, beam energy (GeV), accumulated distance (m),  $\mu_x$  (deg),  $\mu_y$  (deg), number of structures per half-cell and F/D quadrupole gradient (kG/m).
- Penalty function characterizing the quality of matching.
- Summary of ground motion tolerance calculations and other parameters. For example:

```

Ground motion Effects
Uncorrelated quad motion tol[nm]:  73.5462560292435228 7.31074720012235435
Number of quads:  709
Length of quads:  506.150249999990024   Length of linac:  10387.0503299995362
Length of acc:  8954.81999999917389   Energy of acc:  492.515099999973756
Bgrad max:  1300.68862210229668
Dispersive tol[um]:  67.7764034127667543 6.74011598631467379
Wakefield tol[um]:  18.6782875346977626 1.90679483045901255
BNS:  Ncell= 354
Initial Del_bns [%]:  3.11091337746285124 2.88135243980018485

```

The uncorrelated quadrupole motion tolerance above corresponds to induced beam motion with amplitude of 25% of beam size. The dispersive and wakefield tolerances are for 6% emittance growth due to quadrupole and accelerator structure motion, respectively.

The detailed lattice information is stored in the output files described below, where “filename” is the same word as in the name of the input file “linac\_08.filename.input”:

- “linac\_08.filename.mad” contains MAD compatible lattice file.
- “linac\_08.filename.lattice” contains output at every element for the following parameters: element number, accumulated distance (m), element type number, element length (m), quadrupole K-value ( $\text{m}^{-2}$ ) or accelerator gradient (GeV/m), beam energy (GeV),  $\beta_x$  (m),  $\beta_y$  (m),  $\alpha_x$ ,  $\alpha_y$ ,  $\mu_x$  (deg),  $\mu_y$  (deg), BNS autophasing energy spread  $\Delta p/p$ .
- “linac\_08.filename.grad” contains output at every half-quadrupole for beam energy (GeV), accumulated distance (m),  $\beta_x$  (m),  $\beta_y$  (m), number of structures before the half-quad, quadrupole gradient (kG/m).
- “linac\_08.filename.grnd” contains output at every half-quadrupole for beam energy (GeV), accumulated distance (m),  $\beta_x$  (m),  $\beta_y$  (m), number of structures before the half-quad, horizontal and vertical quadrupole motion sensitivities. A tolerance on the motion of an individual quadrupole to limit the ensuing beam motion to 1 sigma of beam size is found by taking the square root of the product of the sensitivity and the beam emittance at the end of the linac.

- “linac\_08.filename.bns” contains output at every half-quadrupole for beam energy (GeV), accumulated distance (m),  $\beta_x$  (m),  $\beta_y$  (m),  $\mu_x$  (deg),  $\mu_y$  (deg), number of structures before the half-quad, horizontal and vertical BNS autophasing energy spread.
- “linac\_08.filename.debug” contains detailed matching output for debugging.
- “linac\_08.filename.bnsx.top” contains “topdraw” file to plot horizontal BNS autophasing energy spread along the linac.
- “linac\_08.filename.bnsy.top” contains “topdraw” file to plot vertical BNS autophasing energy spread along the linac.
- “linac\_08.filename.beta” contains output at every half-quadrupole for accumulated distance (m),  $\beta_x$  (m),  $\beta_y$  (m),  $\mu_x$  (deg),  $\mu_y$  (deg).

### 3 Diagnostic Sections

Because of the long linac length, several diagnostic sections need to be included in the lattice to allow for beam monitoring and correction of machine errors. The optics of diagnostic sections has to be suitable for measurements of beam emittance, energy, energy spread and beam trajectory.

The linac code described in this paper does not automatically include diagnostic sections in the lattice. In the NLC design, we generated the diagnostic sections with MAD, inserted them at desirable locations in the linac and locally matched to the linac optics. Four diagnostic sections had been designed:

1. In the beginning of linac at 10 GeV.
2. After transition between sections 1 and 2 at about 50 GeV.
3. After transition between sections 2 and 3 at about 155 GeV.
4. At the end of linac at 500 GeV.

Each diagnostic section includes 5 identical cells with  $45^\circ$  phase advance and periodic  $\beta$  functions. In addition, sections 1-3 have space for a horizontal chicane to measure beam energy and energy spread. In total, sections 1-to-4 have  $5\frac{1}{2}$ , 7, 7, 6 FODO cells, respectively. To provide space for instrumentation and to prevent interference with the diagnostics, accelerator structures are not included in the diagnostic sections.

The diagnostic sections are locally matched to the linac optics by optimizing 6 quadrupole strengths on each side of the five periodic  $45^\circ$  cells. The use of more than 4 variable strengths allows not only to match the optics to periodic  $\beta$  functions of  $45^\circ$  cells, but also reduce local  $\beta$  distortion and chromatic perturbation.

### 4 Linac Lattice Parameters

The latest lattice files for the NLC main linac can be found at Ref. [7]. The Tables 1-3 show the main lattice parameters of the linac for 500 GeV beams. The linac is divided into 3 sections named Linac-1, 2 and 3, which have 3, 6 and 9 accelerator structures per half-cell, respectively. Each linac section has a diagnostic section at the end. The diagnostic section prior to linac acceleration is not included in these tables.

The  $\beta$  functions along the linac are plotted in Fig. 1. The  $\beta$  amplitude changes from section to section according to the cell length and varies within each section according to phase variation

(Eq. 1). The diagnostic sections have smaller  $\beta$  functions due to shorter cells. The variation of the cell phase advance in the linac is shown in Fig. 2. Fig. 3 shows the linac chromatic bandwidth: BMAG - 1 function vs.  $\Delta p/p$ , which is proportional to chromatic emittance growth after filamentation. The momentum error  $\Delta p/p$  is mainly caused by the phase and accelerating gradient errors in the accelerator structures.

## References

- [1] Y. Nosochkov, “Comparison of Lattice Options for the NLC Main Linac,” LCC-0024 (1999).
- [2] See, for example: T.O. Raubenheimer, “Operation of High-Energy Linacs,” *Handbook of Accelerator Physics and Engineering*, ed.: A. Chao, M. Tigner, p. 252 (1999); or CERN-CLIC-NOTE-347 (1997).
- [3] NLC ZDR Design Group, “Zeroth-Order Design Report for the Next Linear Collider,” SLAC Report 474 (1996); with updated parameters at:  
<http://www-project.slac.stanford.edu/lc/nlc-tech.html>.
- [4] H. Grote, F. C. Iselin, CERN/SL/90-13 (AP) Rev.4 (1994).
- [5] Written by T. Raubenheimer and Y. Nosochkov.
- [6] F.-J. Decker *et al.*, “Status of the SLC Linac,” Proceedings of the EPAC98, Stockholm (1998); or SLAC-PUB-7889 (1998).
- [7] The latest main linac lattice decks were generated by M. Woodley and can be found at:  
“[http://www-project.slac.stanford.edu/lc/local/AccelPhysics/Accel\\_Physics\\_index.htm](http://www-project.slac.stanford.edu/lc/local/AccelPhysics/Accel_Physics_index.htm)”  
under “NLC Optical Lattices”  $\Rightarrow$  “CD1 decks and output”  $\Rightarrow$  “main\_linac”  $\Rightarrow$  “Decks”.

Table 1: Lattice parameters of the NLC main linac.

Parameter	Full linac
Total length (m)	10720.418
Initial energy (GeV)	10
Final energy (GeV)	500
Number of active sectors	46
Number of girders	1656
Girders per sector	36
Number of accelerator structures	4968
Accelerator structures per girder	3
Number of quadrupoles	748
Number of chicane bends	8
Number of regular cells	354
Number of diagnostic sections	3
Number of diagnostic cells	20



Table 2: Lattice parameters of individual linac sections.

Parameter	Linac-1	Linac-2	Linac-3
Total length (m)	976.726	2395.723	7347.969
Initial energy (GeV)	10	52.609	159.130
Final energy (GeV)	52.609	159.130	500
Number of active sectors	4	10	32
Number of girders	144	360	1152
Number of accelerator structures	432	1080	3456
Number of quadrupoles	158	194	748
Number of chicane bends	4	4	0
Number of regular cells	72	90	192
Length of regular cell (m)	12.53966	25.07932	37.61898
Exponential cell phase factor $a$	-0.3	-0.3	0
Initial cell phase $\mu_x/\mu_y$ (deg)	100/105	100/105	85/90
Total number of diagnostic cells	7	7	6
Number of 45° diagnostic cells	5	5	5
Length of 45° diagnostic cell (m)	8.0	16.0	20.0
Length of chicane (m)	11.500953	14.938968	none
Maximum chicane displacement (mm)	18.0	8.5	none
Length of accelerator structure (m)	1.8025		
Accelerator gradient (MeV/m)	54.7191		
Effective bend length (m)	2.65	2.65	none
Bend field (kG)	4.040	4.156	none
Bend angle (mrad)	6.100940	2.075027	none
Number of Q12.75 quads	144	0	0
Number of Q17.00 quads	14	180	0
Number of Q38.25 quads	0	14	396

Table 3: Quadrupole parameters.

Quadrupole	Effective length (m)	Bore radius (mm)	Maximum B'L (kG)	Girders between quads
Q12.75	33.02	6.35	410.0	1
Q17.00	43.82	6.35	550.0	2
Q38.25	97.79	6.35	1380.0	3

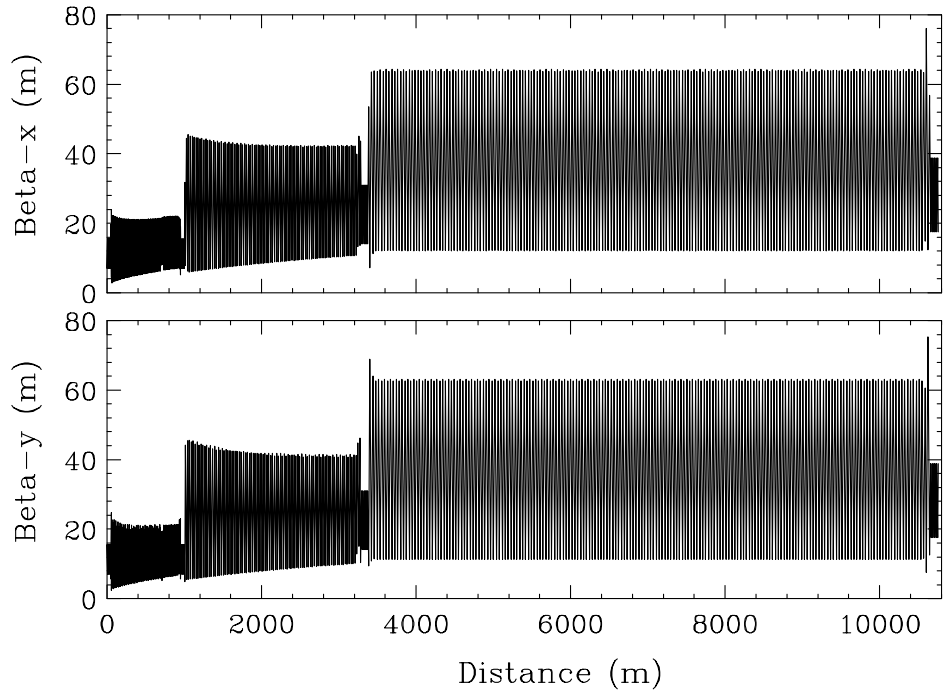


Figure 1:  $\beta$  functions in the linac.

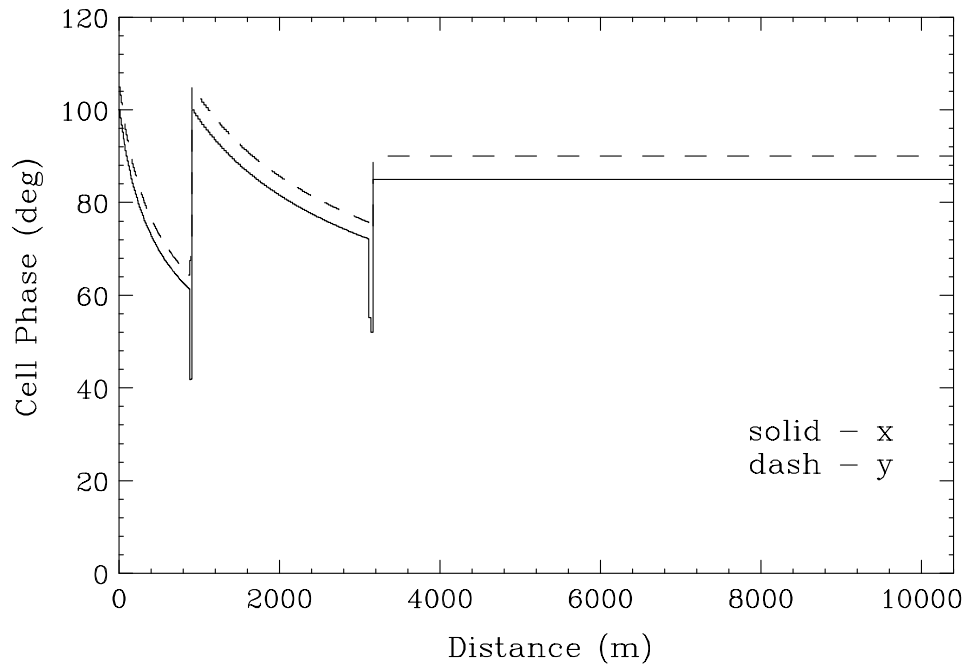


Figure 2: Variation of cell phase advance in the linac.

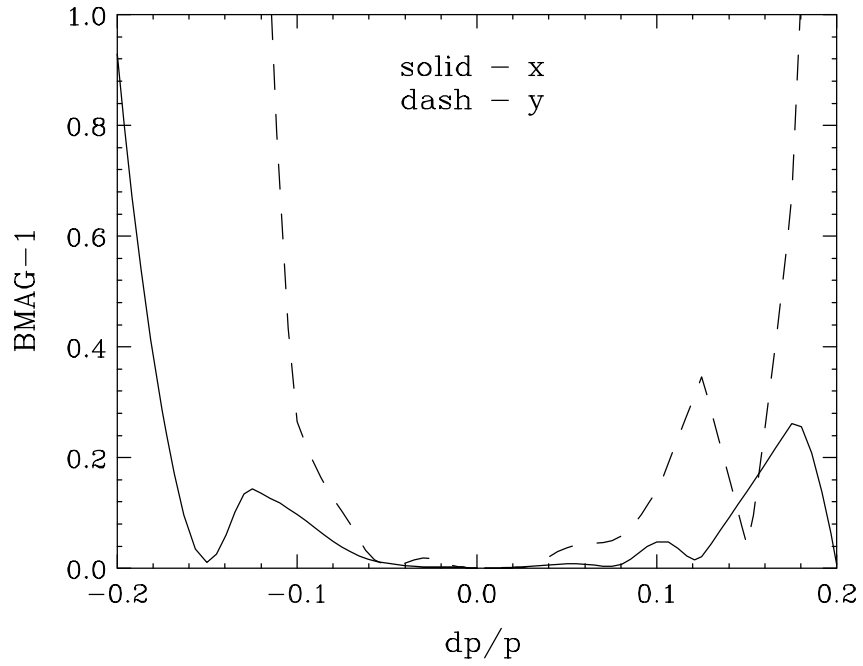


Figure 3: Bandwidth of the linac in terms of BMAG-1 function which is proportional to chromatic emittance growth after filamentation.